Pattern-Based Predictive Control for ETBE Reactive Distillation

Yu-Chu Tian [1], Futao Zhao, B. H. Bisowarno, Moses O. Tadé

Department of Chemical Engineering, Curtin University of Technology, GPO Box U1987, Perth WA 6845, Australia

Abstract

Synthesis of ethyl *tert*-buty ether (ETBE), a high-performance fuel additive, through reactive distillation (RD) is an attractive route, while its operation and control are exceptionally difficult due to its functional combination and complex dynamics. Modern control technology greatly relies on good process models, while a reasonable RD model is too complex for control design. Moreover, RD contains considerable uncertainties that cannot be well described in process modelling. Alleviating the model requirement, this work aims to maintain the product purity in RD of ETBE through developing a pattern-based predictive control (PPC) scheme. Process dynamics, control structure, nonlinear transformation, feature pattern extraction, and pattern-based prediction and its incorporation with a conventional linear controller are discussed. Case studies show the effectiveness of the proposed method.

Key words: reactive distillation, time delay, predictive control, feature patterns, fuzzy logic

1 Introduction

Reactive distillation (RD), a simultaneous implementation of sequential reaction and distillation in a countercurrent column, is an old idea; however, it has received renewed attention in the recent years and is becoming increasingly important in industry [1,2]. It has demonstrated potential improvements in capital productivity and selectivity, and reduction in solvents, energy consumption, and capital investments. Some improvements are dramatic, as described in [2] for a methyl acetate RD process: 5 times lower investment and

[1] Author to whom all correspondence should be addressed. Phone: +61 8 9266 3776, fax: +61 8 9266 2681. E-mail: tiany@che.curtin.edu.au (Y.-C. Tian).

5 times lower in energy consumption by using a hybrid RD process to replace an entire flowsheet with 11 units and related heat exchangers, pumps, intermediate storage vessels, and control systems!

RD is advantageous for a great number of chemical syntheses, including fuel ether production, which is the focus of this work. As fuel additives, fuel ethers have been widely used for improvement of fuel quality. In a continuous effort for development and production of high-performance fuel additives, RD has been successfully applied in the synthesis of the widely used methyl *tert*-butyl ether (MTBE), which has a dual advantage in fuel lead removal and oxygenate introduction.

Current research has focused on MTBE, while recent studies reveal that MTBE has severe water ingress problem that may pollute underground water. Ethyl *tert*-butyl ether (ETBE) has been found to be a potential alternative to MTBE due to its higher performance, less water contamination, and synthesis from semi-renewable products (ethanol from biomass).

RD has been found to be feasible for ETBE production, while the RD of ETBE is still limited worldwide and needs to be commercialised. Moreover, RD involves considerable uncertainties and displays complex behaviour such as high non-linearity, strong interactions, bifurcation and multiplicity, and time delay. RD dynamics and behaviour are yet to be fully understood. Due to the functional integration of reaction and separation, and the dynamics complexity, RD is exceptionally difficult to operate and control. This calls for systematic research on RD process dynamics and control aspects.

The work is done on a pilot-scale RD column for ETBE production at our laboratory. In RD of ETBE, reactant conversion and product (ETBE) purity are two key process variables. The former is a measure of the usage of the raw materials, while the latter characterises the product quality. Both of them are directly related to the productivity of the process. This work will address the maintenance of the purity of product (ETBE), which is withdrawn from the bottom of the RD column.

The ETBE purity will be controlled indirectly by regulating a column temperature. Because the desired purity (purity set-point) may be changed in plant operation, the control system should have a fast set-point tracking ability (tracking problem). On the other hand, RD and other chemical processes always have various disturbances and uncertainties, which cannot be well modelled and predicted, resulting in a requirement of effective disturbance rejection (regulatory problem). Control design should consider both tracking and regulatory problems for RD processes.

A good process model is the basis of modern control technology. Although it is possible to develop a reasonable model for specific RD processes [3,4],

such a model is too complex for control design. Furthermore, RD processes contain a large degree of uncertainties that cannot be well described in process modelling.

To alleviate the model requirement, this work develops a pattern-based predictive control (PPC) scheme incorporating with conventional proportional-integral (PI) controller for the non-linear and complex RD process. Similar ideas have been used for processes with time delay [5]. The process dynamics, control structure, non-linear transformation, and pattern extraction and utilisation for process prediction will be discussed in detail. Case studies will show the effectiveness of the proposed approach.

2 Process Description

The chemical structure of ETBE is $(CH_3)_2COC_2H_5$. It is produced from ethanol and a mixed C_4 olefine stream containing isobutylene (typically of a cracking unit product). The dominant chemical reaction in ETBE synthesis is the reversible reaction of isobutylene and ethanol over an acid catalyst to form ETBE

$$(CH_3)_2C = CH_2 + C_2H_5OH \Longleftrightarrow (CH_3)_3COC_2H_5 \tag{1}$$

The acidic ion-exchange resin, Amberlyst 15, is used in our work. The reaction is equilibrium limited in a range of temperatures. The reaction kinetics has been investigated in [6] and discussed in [3], from where detailed expressions for the equilibrium constant and rate equation are available.

Two side reactions exist in ETBE synthesis. One is the dimerisation of isobutylene to form diisobutylene (DIB) with the chemical structure of $[(CH_3)_2C{=}CH_2]_2$. In the presence of any water in the reaction environment, another side reaction is the hydration of isobutylene to form isobutanol (isobutyle alcohol) with the chemical structure of $(CH_3)_3COH$. The side reactions are expressed by

$$(CH_3)_2C = CH_2 + (CH_3)_2C = CH_2 \Longleftrightarrow [(CH_3)_2C = CH_2]_2 \tag{2}$$

$$(CH_3)_2C = CH_2 + H_2O \Longleftrightarrow (CH_3)_3COH \tag{3}$$

A pilot-scale RD column has been built at our laboratory for ETBE (and MTBE) production. It is graphically shown in Figure 1. With a diameter of 0.155m and a height of 4.1m, the column consists of three sections for rectifying, reaction, and stripping, respectively, and is filled with two novel packings, one of which contains the catalyst, Amberlyst 15, which is necessary

for the etherification reaction. The RD process has a total condenser and a partial reboiler.

The column is estimated to have 8 theoretic stages: 1, 3, and 4 stages in rectifying, reactive, and striping sections, respectively. The condenser and reboiler are considered as two separate stages. Therefore, there are 10 stages altogether, which are numbered from top to bottom as shown in Figure 1. The rectifying section has only one stage (stage 2); the reactive section has 3 stages (stages 3, 4, and 5); and the stripping section has 4 stages (stages 6 to 9). The raw material is fed at stage 6; while the final product, ETBE, is withdrawn from stage 10 (reboiler). Measurement points are also indicated in Figure 1 for temperature, flow rate, pressure, and level variables. More information about the the architecture of the RD process can be found in [3,4,7].

A typical set of operating conditions of the RD process for ETBE synthesis is tabulated in Table 1. It will be considered as the nominal situation, at which the control system for the ETBE purity will be designed.

3 Control System Configuration

RD control is challenging due to high non-linearity, strong interactions, bifurcation and multiplicity, time delay, process uncertainties, and the large number of possible control configurations. From the control point of view, an RD process has 5 degrees of freedom for control design, i.e. 5 process variables can be manipulated (control inputs): flow rates of reflux(L), boil-up (V), distillate (D), bottoms (B), and column top vapour V_T. The reflux ratio L/D can be used instead of L for control design. In our pilot-scale RD process, the flow rates of boil-up (V) and column top vapour (V_T) are characterised by reboiler duty (Q_r) and condenser duty (Q_c). The controlled variables (control objectives) are reflux accumulator and reboiler levels, column pressure, bottoms (ETBE) purity, and reactant conversion. Typical disturbances to the RD process include changes in feed composition (F_c), which is characterised by the stoichiometric ratio, and in feed flow rate (F_f).

In practice, three control loops are designed for inventory and pressure control. The control configuration problem addressing which of the five degrees of freedom should be used in those three loops has been extensively discussed, e.g. [8]. Two more loops can be designed for purity and conversion control. The resulting control configuration is conventionally named by the two independent variables that are used for composition (purity) control, e.g. LV, LB, D/V, (L/D)(V/B), etc. Among all possible control structures including ratio schemes and those with consideration of feed flow rate F_f, non-ratio schemes LV and LB has been shown to be preferred for the RD column under

consideration [4]. This work will consider the LV configuration.

In the LV configuration of the RD process, the column pressure is maintained by manipulating the condenser duty Q_c; the inventory control for reflux accumulator and reboiler hold-up is implemented by adjusting the distillate flow rate D and bottoms flow rate B, respectively. The reflux flow rate L is fixed while the reboiler duty Q_r is manipulated for product (ETBE) purity. This is a typical one-point control problem in RD processes.

The purity control is important, while it is not easy because the purity characterised by composition is difficult to measure in real time reliably and economically. Fast and reliable measurement of the controlled variable is a basic requirement of closed-loop control.

A method to overcome this difficulty is to implement inferential control for the purity. In this method, an inferential model has to be developed to infer the purity from multiple measurements that are easily obtained, e.g. multiple column temperatures. Progress has been made in this direction [9,7].

An alternative method to overcome the difficulty is to indirectly control the purity by controlling some other process variables that are easy to obtain and are indicators of the purity. However, such indicators are not easy to find due to the unavailability of a one-to-one relationship between a single variable and the purity. In distillation column control practice, column temperatures are usually used for indirect composition control.

The reboiler temperature reflects the dynamic changes of the ETBE purity quickly, while it is not a good purity indicator since a single reboiler temperature value may correspond to multiple purity values [7]. In this work, the stage 7 temperature T_7 is used for inference and control of the product (ETBE) purity for the RD process under consideration.

4 Process Dynamics

The steady state relationship between the ETBE purity and the reboiler duty Q_r for a fixed reflux flow rate is shown in Figure 2 [7]. $Q_r = 8.45$kW is around an optimal Q_r value that gives the maximum value of the ETBE purity. It is chosen as the nominal operating point.

The steady state relationships between T_7 and Q_r are investigated under different reflux flow rates and are graphically depicted in Figure 3. It is clearly seen from Figure 3 that there exists a significant non-linearity in process gain k_p (k_p is high within an operating range of Q_r but becomes small outside this

range), and the reflux flow rate L affects the T_7 versus Q_r relationship in a complex manner.

The ETBE purity versus Stage 7 temperature T_7 can be easily obtained from Figures 2 and 3. Although the relationship between T_7 and the ETBE purity is non-linear, T_7 determines the purity uniquely. Another advantage of using T_7 is that the sensitivity of T_7 to the purity is high [4].

It has been found that the RD process has changeable inertia as operating conditions change, suggesting time-varying process response speed. By convention, the inertia is characterised by a time constant or multiple time constants.

Detailed investigation also reveals considerable time delay from Q_r to T_7, implying that any manipulation in Q_r will not affect T_7 until the time delay elapses. The significance of the RD time delay is shown in Table 2. The existence of time delay imposes severe constraints on the control system and complicates the control system design.

With a fixed heat input to the reboiler, an increase in feed flow rate F_f will result in an increase in bottoms flow rate and consequently a decrease in the temperatures below column stage 6. On the other hand, the feed stoichiometric ratio characterising the feed composition has a positive effect on T_7, i.e. an increase in the ratio will lead to an increase in T_7. Changes in feed flow rate F_f and feed composition F_c are primary disturbances to the process operation. These disturbances affect T_7 dynamics significantly in a complex manner, e.g. nonlinear gain, time-varying inertia, and time delay, which are similar to but different in value from those from Q_r to T_7.

Simplified input-output process models expressed by transfer functions for manipulation and disturbances are identified under specific operating conditions. The identified results are first-order plus time delay descriptions, which are tabulated in Table 2. Table 2 shows the RD process dynamics quantitatively. For example, the process gain, time constant, and time delay all change in a wide range as process operating conditions change. While more complex expressions of T_7 dynamics can be precisely established from the first principles of mass balance and energy balance, e.g. [3,4], these types of models are difficult to use for control design.

5 Pattern-Based Predictive Control

Due to the complexity of the RD process dynamics, conventional control technologies, e.g. PI control, cannot provide satisfactory control performance,

while the application of modern control technology requires good process models. A reasonable process model as described in [3,4] contains hundreds of equations for the 10-stage RD process under consideration. It is too complicated to be directly used for control system design. Simplified input-output process models discussed in the last section are helpful in understanding the complex process dynamics, but they are identified under some specific operating conditions and thus cannot represent the process in a wide range of operating conditions. Although it is possible to extend the transfer function models, again this will complicate the control system design. Furthermore, the RD process contains a large degree of uncertainties, which cannot be well described using any type of mathematical expressions. Therefore, techniques without using exact process models are more attractive for RD control.

Pattern-based predictive control (PPC) is such a method that does not rely on exact process models while providing improved control performance for complex processes over conventional, e.g. PI, control algorithms. Some progress has been made in this direction, e.g. for time delay compensation [5], adaptive PI [10], fuzzy predictive control [11], etc.

The proposed PPC system for the RD process is schematically depicted in Figure 4, which is a further development of the authors' previous work [5] that considers linear processes. It consists of two main parts: a non-linear transformation $u = f(v)$ and a pattern-based predictor (PP). The former is used for input-output linearisation of the process gain, while the latter is employed to anticipate process output some (e.g. d) steps ahead. The PP utilises process feature patterns qualitatively and quantitatively, which are extracted from the controlled and manipulated variables, and is incorporated with a conventional controller G_c (e.g. PI) in the PPC system. For the RD system, y and u in Figure 4 correspond to T_7 and Q_r, respectively.

Ideally, The PP acts as a time lead component as it provides d steps ahead prediction of the controlled variable. It will effectively compensate for the time delay in the the RD process and thus allows more aggressive controller settings compared with the control systems without PP. Therefore, the PPC will provide improved performance in both set-point tracking and disturbance rejection, as will be shown later for the RD process.

The nonlinear transformation, feature pattern extraction, and PP design will be respectively discussed in the successive sections.

6 Nonlinear Transformation

Because the process has a highly nonlinear process gain, which will degrade the prediction performance of the PP, a nonlinear transformation

$$u = f(v) \tag{4}$$

is introduced to obtain a $v \sim y$ relationship with a pseudo linear gain, where v is the new manipulated variable. This is a type of input-output linearisation [12], which is one of the most widely used techniques for nonlinear control system design.

Notice that controlling a process always requires a certain degree of understanding of the process. The rough knowledge of the process gain can be obtained *a priori*, which is sufficient to construct such a nonlinear transformation. Moreover, a linear PP can accommodate a certain degree of process uncertainties, implying that no exact nonlinear transformation is required.

The process gain k_p can be determined by the derivatives of the curves in Figure 3. Let $g(u)$ denote the steady state input-output relationship of Figure 3, i.e.

$$y = g(u) \tag{5}$$

Ideally, $f(v)$ is designed such that y is linear to the new manipulated variable v, i.e.

$$y = g[f(v)] = bv + c \tag{6}$$

where b is a constant representing the gain of the input-output linearised system; c is also a constant representing the bias. It follows that $f(v)$ is the inverse of $g(bv + c)$, i.e.

$$f(v) = g^{-1}(bv + c) \tag{7}$$

The determination of the constants b and c is straightforward and can be done at the operating point of the RD process. Tables 1 and 2 shows that at the operating point, $Q_r = 8.45$kW, $T_7 = 133.12°$C, $k_p = 49.28°$C/kW. Suppose that these values are retained in the input-output linearised system. According to equation (6), we have

$$b = 49.28, c = -283.2960 \tag{8}$$

The solid curve of Figure 3 corresponds to the nominal operating conditions of the RD process. From this curve, the following nonlinear transformation function $f(v)$ can be constructed

$$f(v) = p_1 + p_2 \exp\left[p_3(bv + c - p_4)\right] + p_5 \ln(bv + c),\ v \in [7.4, 8.6] \quad (9)$$

where $p_1 \sim p_5$ are parameters, which are taken to be

$$[p_1, \cdots, p_5] = \begin{cases} [5.0786, -1, -0.9837, 83.3992, 0.6813], & v \leq 8.0993; \\ [3.5615, 1, 0.5623, 140.083, 1], & \text{otherwise} \end{cases} \quad (10)$$

As shown in equation (9), under the nominal operating conditions, v is limited within [7.4,8.6], resulting in a range of [6.6,10.6]kW for u. Computation of the designed nonlinear transformation $f(v)$ shows that $8.45 \approx f(8.4196)$, implying that the nominal value of v is 8.4196, which has a small deviation from the nominal value of u (8.45kW). The designed $u = f(v)$ versus v is shown in Figure 5, in which a portrait of y versus v is also depicted. As expected, a pseudo linear relationship between y and v is obtained within $v \in [7.4, 8.6]$.

7 Selection and Extraction of Feature Patterns

Instead of using an exact process model, a PPC system utilises process feature patterns qualitatively and quantitatively for process prediction. Therefore, selection and extraction of process feature patterns are crucial in PPC design.

In process control systems, the controlled variable y is measurable and the manipulated variable u can be recorded from the controller output. Therefore, the time series $\{y(k)\}$ and $\{u(k)\}$ are available for real-time process analysis and control. The process feature patterns are extracted from these two time series. The basic ideas of the feature pattern extraction have been discussed by the authors [5] and will be further developed below.

Most chemical processes behave with an S-shaped response to a step change in either manipulated variable or disturbances, as shown in Figure 6. The response can be characterised by four stages with different dynamic behaviour. The first stage is the *time delay* stage, in which the process accumulates energy or materials while without any response to the input. Right after the time delay elapses is the the second stage, the *accelerating increase stage*, in which the process starts to respond to the input with an accelerating rate due to the "energy-storing" effect of the first stage. The third stage, the *decelerating increase stage*, starts from an inflection point of the response, which remains increasing yet with a decreasing rate due to the "energy-releasing"effect. The

process response increases until it finally reaches a steady state, which is the last stage of the response.

The difference between the values of the controlled variable at two successive sampling instants captures the incremental variation of the controlled variable. Thus, the following process feature pattern, S_1, is extracted from the time series of the controlled variable

$$S_1(k) = y(k) - y(k-1) \tag{11}$$

For a step change excitation, $S_1 = 0$ implies that the response is either in *time delay* stage or in *steady state* stage. Instead of using the equality $S_1 = 0$, the inequality $|S_1| < \epsilon$ should be used in practice in order to accommodate any types of noises, where $\epsilon > 0$ is a small and predetermined threshold.

It is easy to know that S_1 cannot discriminate between the *accelerating* and *decelerating increase* stages of the process response to a step change excitation as S_1 gives the same sign in both stages. This difficulty can be overcome by introducing some sort of S_1 variation as a process feature pattern, which is denoted by S_2

$$S_2(k) = \begin{cases} 0, & |S_1(k)| < \epsilon; \\ \dfrac{1}{d} \displaystyle\sum_{m=1}^{d} \left[S_1(k+1-m) - S_1(k-m) \right], & \text{otherwise} \end{cases} \tag{12}$$

where d is the prediction horizon and satisfies

$$d \geq \theta / T_s \tag{13}$$

where θ and T_s are process time delay and sampling period, respectively.

S_2 captures the fluctuating trends of S_1 in the *accelerating* and *decelerating increase* stages of the process response to a step change excitation. $S_2 > 0$ and $S_2 < 0$ imply that the response increases with an increasing and decreasing rates, respectively.

It is helpful to conceptually consider the feature patterns S_1 and S_2 as the first- and second-order differences in discrete-time systems, compared with the first- and second-order derivatives in continuous-time systems.

Time delay is a common phenomenon in chemical processes. Materials and energy fed to a process will not affect the process output within the *time delay* stage of the process response, while they will eventually change the controlled

variable in the later stages. Therefore, the time series of the manipulated variable also contain information of the future process output.

Instead of the real manipulated variable u, the transformed manipulated variable v will be used in feature pattern extraction. The magnitude of v is already reflected in the feature patterns S_1 and S_2, while the incremental variation of v characterising additional excitation has not been covered by either S_1 or S_2. The following feature pattern S_3 captures the incremental variation of v during the time period $[k-d, k]$

$$S_3 = \sum_{m=1}^{d} [v(k+1-m) - v(k-d)] \tag{14}$$

In geometry, S_3 reflects the area bounded by the curve $v(k)$ and the straight line crossing the point $(k-d, v(k-d))$ over the time period $[k-d, k]$. It influences the process output in a complex manner, which needs more feature patterns to characterise. The following feature pattern S_4 can assist in determining the effect of S_3 on the process output.

$$S_4 = \begin{cases} 0, & |S_3(k)| < \epsilon; \\ \left| \dfrac{1}{S_3} \displaystyle\sum_{m=1}^{d} m[v(k+1-m) - v(k-d)] \right|, & \text{otherwise} \end{cases} \tag{15}$$

8 Pattern-Based Fuzzy Prediction

The d steps ahead prediction of the controlled variable is carried out using the following simple formulae, which are based on the extracted process feature patterns

$$\hat{y}(k+d|_k) = y(k) + \Delta\hat{y}(k+d|_k) \tag{16}$$

$$\Delta\hat{y}(k+d|_k) = r_1 [S_1(k) + r_2 S_2(k)] + r_3(k) S_3(k) + h(k)\Delta\hat{y}(k|_{k-d}) \tag{17}$$

where $r_1 \sim r_3$ are three coefficients; $h > 0$ is an updating factor for real-time adaptation.

h can be simply chosen to be a constant, implying that a fixed step is used. The following variable step algorithm is employed in this work for updating h

$$h(k) = h(k-1) + \Delta h(k) \tag{18}$$

where $\Delta h(k)$ is designed to be 0 if $|\Delta\hat{y}(k|_{k-d})| < 0.001$, and $0.01|\Delta\hat{y}(k|_{k-d})|$

if $|\Delta\hat{y}(k|_{k-d})| > 0.1$ and $|\Delta\hat{y}(k|_{k-d}) - \Delta\hat{y}(k-1|_{k-d-1})| < 0.001$. For all other conditions, take $\Delta h(k) = 0.01\text{sign}\left[\Delta\hat{y}(k|_{k-d}) - \Delta\hat{y}(k-1|_{k-d-1})\right]\Delta\hat{y}(k|_{k-d})$.

The determination of the values of the parameters r_1 and r_2 relies on an estimate of the ratio T/θ. However, r_1 and r_2 are fixed for a specific value of T/θ. They should be proportional to the prediction horizon d and should be a function of the ratio T/θ. The following heuristic relations can be used to determine r_1 and r_2

$$r_1/d = 0.6622 + 0.0244(T/\theta) - 0.5482\exp\left(-2.1T/\theta\right) \tag{19}$$
$$r_2/d = 0.2039 + 0.0047(T/\theta) - 0.1797\exp\left(-2T/\theta\right) \tag{20}$$

Equation (20) has extended the guideline for r_2 determination in a table form in [5], where the parameter r_2 was integrated into the feature pattern S_2.

A compact, explicit, and satisfactory expression for r_3 has not been established due to the complex influences of the feature patterns S_3 and S_4 on the process output. However, our experience tells us that r_3 should be determined based on the ratio T/θ and the feature pattern S_4. Therefore, a set of fuzzy logic rules is developed to describe r_3 qualitatively and quantitatively.

Let FS_x denote the fuzzy set of the variable $x \in \{T/\theta, S_4, r_3\}$. Each of the three fuzzy sets uses three linguistic terms: big (B), medium (M), and small (S), to represent, in an approximate and quantised way, the magnitude of the corresponding variable. Let $A_x^i \in \{B, M, S\}$ denote a specific linguistic value of FS_x in the ith fuzzy rule, $x \in \{T/\theta, S_4, r_3\}$. The triangle membership function, denoted by $\mu(\cdot) \to [0, 1]$, is used for the fuzzy sets $FS_{T/\theta}$ and FS_{S_4}, as shown in Figure 7.

Corresponding to $A_{r_3}^i \in \{B, M, S\}$, three central numerical values denoted by $V(A_{r_3}^i)$ can be identified using, say, the least-squares technique. The fuzzy logic rules take the If-Then form, e.g.

$$\text{R}^i\text{: } \textbf{If } \left(T/\theta \text{ is } A_{T/\theta}^i\right) \text{ and } \left(S_4 \text{ is } A_{S_4}^i\right) \textbf{ Then } r_3 \text{ is } V\left(A_{r_3}^i\right) \tag{21}$$

Combining $FS_{T/\theta}$ and FS_{S_4}, 5 fuzzy rules are designed, which are tabulated in Table 3. These rules are schematically depicted in Figure 7. The computation of the degrees of fulfillment for these rules is also shown in Table 3 [13]

Finally, the parameter r_3 is computed over the entire fuzzy rules using the following defuzzification formula

$$r_3(k) = \sum_{i=1}^{5}\left[\beta_i V\left(A_{r_3}^i\right)\right] / \sum_{i=1}^{5}\beta_i \tag{22}$$

It is worth mentioning that for a specific application, if T/θ is not time-varying, the number of rules, and thus the number of β_i in Table 3, will be reduced to 3, as will be discussed in the case studies in the next section.

9 Case Studies

9.1 System Configuration

The developed pattern-based predictive control (PPC) strategies are used for purity maintenance in RD of ETBE. The purity is controlled indirectly by controlling the stage 7 temperature T_7 of the RD column; while T_7 is maintained by manipulating the reboiler duty Q_r. This is a one-point control problem in RD.

For the RD process under consideration, as shown in Table 2, $T = 15.6$min and $\theta = 7$min under the nominal operating conditions. T_s and ϵ are set to be 1min and 10^{-5}, respectively. According to equation (13), set $d = 8$. The initial value of h is taken to be 0.1.

For process prediction using equation (17), r_1, r_2, and r_3 are required. Equations (19) and (20) give $r_1 = 5.6919$ and $r_2 = 1.6983$. r_3 is obtained through fuzzy logic inference.

For the specific RD control problem, $T/\theta = 15.6/7$ is already known, which is *Big* with $\mu\,(T/\theta \text{ is } B) = 1$ as shown in Figure 7. Therefore, the rules R^3 and R^5 in Table 3 are excluded and the remaining rules R^1, R^2, and R^4 are simplified to

$$\begin{aligned} &\mathrm{R}^1\text{: } \textbf{If } (S_4 \text{ is } B) \ \textbf{ Then } r_3 \text{ is } V(S) \\ &\mathrm{R}^2\text{: } \textbf{If } (S_4 \text{ is } M) \ \textbf{Then } r_3 \text{ is } V(M) \\ &\mathrm{R}^4\text{: } \textbf{If } (S_4 \text{ is } S) \ \textbf{ Then } r_3 \text{ is } V(B) \end{aligned} \tag{23}$$

which correspond to the first row of Figure 7. Consequently, β_1, β_2, and β_4 in Table 3 are reduced to

$$\beta_1 = \mu(S_4 \text{ is } S),\ \beta_2 = \mu(S_4 \text{ is } M),\ \beta_4 = \mu(S_4 \text{ is } S) \tag{24}$$

Taking into account Figure 7, the computation of equation (24) is shown in Table 4.

It is seen from Table 4 that $\beta_1 + \beta_2 + \beta_4 = 1$ for any specific values of S_4, implying that equation (22) for r_3 computation is reduced to

$$r_3 = \beta_1 V(S) + \beta_2 V(M) + \beta_4 V(B) \tag{25}$$

As also shown in Table 4, the relationship in equation (25) can be further simplified for specific values of S_4 due to the fact that one or more $\beta_i = 0$. Three values of $V(B)$, $V(M)$, and $V(S)$ have been identified to be 2.4510, 1.0622, and -1.9974, respectively.

Typical curves of $v(t)$, $y(t)$, $\hat{y}(t|t - dT_s)$, $y(t) - \hat{y}(t|t - dT_s)$, $h(t)$, and $S1$ to S_4 are shown in Figures 8, 9, and 10. It is seen from these figures that the d steps ahead prediction of y matches the real y very well, and the prediction error is within ± 1.5°C ($\pm 1.25\%$ of the real y) for the v with gradual and sharp changes. h is updated if prediction error exists, as shown in Figure 9. However, in this example, h (< 0.21) contributes at most 0.26°C to the prediction, implying that the adaptive term, i.e. the last term of equation (17), weighs about $0.26/133 \approx 0.2\%$ of the total predicted quantity and is actually negligible. Thus, the prediction is mainly based on the feature patterns S_1 to S_4 shown in Figure 10.

The PP is incorporated with a conventional PI controller, which is tuned for set-point tracking for the index of the integral of time-weighted absolute error (ITAE). The controller settings are $k_c = 0.1331$ and $T_i = 22.1$min. Those settings can ensure the control performance and stability in a wide range of operating conditions.

The performance of the PPC is evaluated and compared with that of a direct PI control for the RD column. Both setpoint tracking and disturbance rejection responses will be considered. The direct PI controller is also tuned in the range of operating conditions for set-point tracking for the ITAE index, resulting in more conservative settings $k_c = 0.0203$ and $T_i = 19.9$min, compared with the PI controller settings in the PPC system.

9.2 Set-Point Tracking

For set-point tracking, a -5°C step change and a $+2$°C ramp change in T_7 setpoint are introduced at time instants 50min and 150min, respectively. The control results are given in Figure 11, which shows that less overshoot and shorter settling time are obtained from the PPC system. The PPC system improves the ITAE index by over 25% over the direct PI control system, as shown in Table 5.

9.3 Rejection of Feed Composition Disturbances

Changes in feed composition, which is represented by the stoichiometric ratio, are disturbances to the RD column. ±5% (i.e. ±0.25) step changes in feed composition are introduced to the process in order to test the disturbance rejection ability of the PPC system. The step changes occur at the time instants 50 and 150min, respectively. Figure 12 depicts the control results, which show that PPC provides significant improvement over the disturbance rejection ability. The ITAE index improvement reaches over 50%, as shown in Table 5.

9.4 Rejection of Feed Rate Disturbances

Changes in feed flow rate are also disturbances to the RD column. ∓10% (i.e. ±0.074L/min) step changes in feed flow rate are introduced at the time instants 50 and 300min, respectively. The control results are illustrated in Figure 13, which shows that disturbances in feed flow rate have severe effect on the RD process. The PPC system outperforms the direct PI control system as it rejects the disturbances much more effectively with much smaller ITAE indices (the improvement $> 55\%$), as shown in Figure 13 and Table 5. Some sort of ratio control involving the feed flow rate is an option for conventional PI control to improve the disturbance rejection performance, while previous studies have provided no incentive to configure a ratio control system in the studied RD column [4].

9.5 Remarks

It is worth mentioning that the RD process is severely nonlinear. Therefore, system analysis and performance evaluation have to be made at the specific operating point. The nominal RD operating condition for this work is clearly listed in Table 1. Since this work addresses one-point control (purity control of the bottoms product), the reflux flow rate has been fixed at 2.53L/min. As a result, the degree of process nonlinearity is reduced. This is why the performance of the direct PI control is also acceptable in the case studies, although the PPC system does provide improvement over the direct PI control.

Through manipulating the reboiler duty Q_r, the stage 7 temperature T_7 is controlled as the indicator of the bottoms product purity. As shown in Table 1 , the nominal value of the purity is 90mol%. The relationship between the purity and T_7 can be easily obtained from Figures 2 and 3.

10 Conclusions

RD of ETBE is a non-conventional and complex process with high nonlinearity, strong interactions, bifurcation and multiplicity, time delay, and large degree of process uncertainties. A PPC system has been developed for the purity of a pilot-scale RD process for ETBE synthesis. Alleviating the requirement of good process models, which are essential for modern model-based control, it utilises feature pattern-based prediction incorporated with conventional PI control. To obtain a pseudo input-output linear process gain, a nonlinear transformation is designed, which needs only a rough and easily obtained knowledge of the steady state characteristics of the process. Four types of process feature patterns are extracted from the time series of the controlled variable and the transformed manipulated variable. Fuzzy logic rules driven by the extracted feature patterns are then developed for process prediction. Case studies have shown that the PPC can provide improved control performance for both set-point tracking and disturbance rejection. The PPC is a promising tool for complex processes, where good process models are difficult to obtain or to implement for real-time control.

Acknowledgements

The authors would like to thank Australian Research Council (ARC) for its support under large and small grant schemes (ARCLGS and ARCSGS). The first author (YCT) also acknowledges the supports from Western Australia state government under strategic research fellowships, and Curtin University of Technology under research grant schemes (CUTRGS) and small discovery grants schemes.

Nomenclature

A_x^i	$\in \{B, M, S\}$: a linguistic value of FS_x for the ith rule, $x \in \{T/\theta, S_4, r_3\}$
β_i	Degree of fullfillment for the ith rule
B	Bottoms flow rate (L/min), or the linguistic term "Big"
$b,\ c$	Constants in the nonlinear transformation
$\Delta\hat{y}$	d steps ahead prediction of the y deviation
D	Distillate flow rate (L/min)
d	Number of prediction steps
ϵ	Small and positive threshold in S_2
f	Nonlinear transformation within the PPC system
F_c	Feed composition (stoichiometric ratio)

F_f Feed flow rate (L/min)
FS_x Fuzzy set of the subscript variable $x \in \{T/\theta, S_4, r_3\}$
g Intermidiate function, at steady state $y = g(u)$
G_c Controller
G_L Process transfer function in disturbance path
G_p Process transfer function in manipulation path
h Updating factor for process prediction
k Present sampling instant
k_c controller gain
k_p Process gain (°C/kW)
L Reflux flow rate (L/min) or Load
M The linguistic term "Medium"
μ Membership function
$p_1 \sim p_5$ Parameters for nonlinear transformation f
Q_c, Q_r Condenser duty and reboiler duty (kW)
R Setpoint
$r_1 \sim r_3$ Parameters for prediction of the controlled variable
S The linguistic term "Small"
$S_1 \sim S_4$ Process feature patterns
T Process time constant
T_7 Stage 7 temperature (°C)
T_i Controller integral time (min)
θ Process time delay (min)
T_s Sampling period (min)
u Manipulated variable (e.g. reboiler duty)
V Boilup flow rate (L/min)
v Transformed manipulated variable within the PPC system
$V\left(A^i_{r_3}\right)$ Central numerical values of $A^i_{r_3} \in \{B, M, S\}$
V_T Column top vapour flow rate (L/min)
y Controlled variable (e.g. stage 7 temperature)
$\hat{y}$ d steps ahead prediction of y

References

[1] M.F. Malone and M.F. Doherty. Reactive distillation. *Ind. Eng. Chem. Res.*, 39:3953–3957, 2000.

[2] R. Taylor and R. Krishna. Modelling reactive distillation. *Chem. Eng. Sci.*, 55(2):5183–5229, 2000.

[3] M.G. Sneesby, M.O. Tadé, R. Datta, and T.N. Smith. ETBE synthesis via reactive distillation. 1. steady state simulation and design aspects. *Ind. Eng. Chem. Res.*, 36:1855–1869, 1997.

[4] M.G. Sneesby, M.O. Tadé, R. Datta, and T.N. Smith. ETBE synthesis via reactive distillation. 2. dynamic simulation and control aspects. *Ind. Eng. Chem. Res.*, 36:1870–1881, 1997.

[5] F. Zhao, J. Ou, and W. Du. Pattern-based fuzzy predictive control for a chemical process with dead time. *Eng. Appl. of Artificial Intelligence*, 13(1):37–45, 2000.

[6] K.L. Jensen and R. Datta. Ethers from ethanol. 1. equlibrium thermodynamic analysis of the liquid phase ethyl *tert*-butyl ether reaction. *Ind. Eng. Chem. Res.*, 34:392–399, 1995.

[7] Y.C. Tian and M.O. Tadé. Inference of conversion and purity for ETBE reactive distillation. *Brazilian J. of Chem. Eng.*, 17:617–625, 2000.

[8] S. Skogestad, P. Lundström, and E.W. Jacobsen. Selecting the best distillation control configuration. *AIChE J.*, 36(5):753–764, 1990.

[9] M.G. Sneesby, M.O. Tadé, and T.N. Smith. Two-point control of a reactive distillation column for composition and conversion. *J. Process Control*, 9(1):19–31, 1999.

[10] J.E. Seem. A new pattern recognition adaptive controller with application to HVAC systems. *Automatica*, 34(8):969–982, 1998.

[11] M.J. Jang and C.L. Chen. Fuzzy successive modelling and control for time-delay system. *Int. J. System Science*, 27(12):1483–1490, 1996.

[12] C. Kravaris and C.J. Kantor. Geometric methods for nonlinear process control: 1. background; 2. controller synthesis. *Ind. Eng. Chem. Res.*, 29(12):2295–2323, 1990.

[13] R. Babuška. An overview of fuzzy modeling and model-based fuzzy control. In H.B. Verbruggen and R. Babuška, editors, *Fuzzy Logic Control Advances in Applications*, pages 3–35. World Scientific, 1999.

Captions of Illustrations

Figure 1: Pilot-scale RD column (T, F, P, L in dashed circles mean measurements for temperature, flow rate, pressure, and level variables).

Figure 2: Purity and Conversion versus reboiler duty for the reflux fixed at 2.53L/min.

Figure 3: Stage 7 temperature T_7 versus reboiler duty Q_r.

Figure 4: PPC system structure.

Figure 5: Nonlinear transformation and the resulting y versus v relationship.

Figure 6: S-shape process response to a step change in either the manipunated variable or disturbances. I: time delay stage; II: accelerating increase stage; III: decelerating increase stage; IV: steady state stage; A: inflection point.

Figure 7: Fuzzy sets and fuzzy rules.

Figure 8: Typical curves of v, y, and $\hat{y}$.

Figure 9: Typical $y(t) - \hat{y}(t|t - dT_s)$ and h curves corresponding to Figure 8.

Figure 10: Typical curves of S_1 to S_4 corresponding to Figure 8.

Figure 11: Setpoint tracking.

Figure 12: Rejection of $\pm 5\%$ disturbances in feed composition.

Figure 13: Rejection of $\mp 10\%$ disturbances in feed flow rate.

Table 1
A typical set of RD operating conditions.

Feed composition		
ETBE	29.1	mol%
Ethanol	9.1	mol%
Isobutylene	7.3	mol%
n-Butylene	54.5	mol%
Stoichiometric excess ethanol	5.0	mol%
Feed rate	0.76	L/min
Distillate rate	0.50	L/min
Reflux flow rate	2.53	L/min
Bottoms rate	0.53	L/min
Overhead pressure	950	kPa
Bottoms ether purity	90	mol%
Reboiler duty	8.45	kW
Reboiler temperature	160	°C
Stage 7 temperature	133.12	°C

Table 2
First-order plus delay dynamics of T_7 versus Q_r.

L	Q_r	k_p	T	d
L/min	kW	°C/kW	min	min
2.30	8.10	19.25	3.04	4.09
	8.45	3.40	1.41	2.38
	8.75	3.31	3.7	2.19
2.40	8.10	209.23	32.50	1
	8.45	4.87	3.04	4.09
	8.75	4.22	4.9	2.56
2.53	8.10	35.34	60.00	0
	8.45	49.28	15.60	7.0
	8.75	4.29	7.6	2.93
Disturbances				
+5% change in F_f		2.88	16	2
−5% change in F_f		2.88	18	2
+5% change in F_c		−30.36	38	0
−5% change in F_c		−30.60	40	5

Table 3
Fuzzy rules and degrees of fullfillment.

R^i	IF	THEN	β_i
R^1	S_4 is B	r_3 is S	$\beta_1 = \mu(S_4 \text{ is } S)$
R^2	$(T/\theta$ is not $S)$ and $(S_4$ is $M)$	r_3 is M	$\beta_2 = \min\{1 - \mu(T/\theta \text{ is } S), \mu(S_4 \text{ is } M)\}$
R^3	$(T/\theta$ is $S)$ and $(S_4$ is $M)$	r_3 is S	$\beta_3 = \min\{\mu(T/\theta \text{ is } S), \mu(S_4 \text{ is } M)\}$
R^4	$(T/\theta$ is $B)$ and $(S_4$ is $S)$	r_3 is B	$\beta_4 = \min\{\mu(T/\theta \text{ is } B), \mu(S_4 \text{ is } S)\}$
R^5	$(T/\theta$ is not $B)$ and $(S_4$ is $S)$	r_3 is M	$\beta_5 = \min\{1 - \mu(T/\theta \text{ is } B), \mu(S_4 \text{ is } S)\}$

Table 4
Degrees of fullfillment and r_3 for the RD purity control.

S_4	≤ 2.4	$(2.4, 4.0]$	$(4.0, 5.6]$	> 5.6
$\beta_1 = \mu(S_4 \text{ is } S)$	1	$2.5 - S_4/1.6$	0	0
$\beta_2 = \mu(S_4 \text{ is } M)$	0	$S_4/1.6 - 1.5$	$3.5 - S_4/1.6$	0
$\beta_4 = \mu(S_4 \text{ is } B)$	0	0	$S_4/1.6 - 2.5$	1
r_3	$V(S)$	$\beta_1 V(S) + \beta_2 V(M)$	$\beta_2 V(M) + \beta_4 V(B)$	$V(B)$

Table 5
Comparisons of ITAE indices.

Magnitude	Period	Direct PI	PPC	Improve.
-5°C step in T_7	50-150min	657	479	27.1%
$+2$°C ramp in T_7	150-300min	434	313	27.9%
$+5$% step in F_c	50-150min	2529	1167	53.9%
-5% step in F_c	150-300min	2967	1175	60.4%
-10% step in F_f	50-300min	2461	1077	56.3%
$+10$% step in F_f	300-600min	2737	1210	55.8%

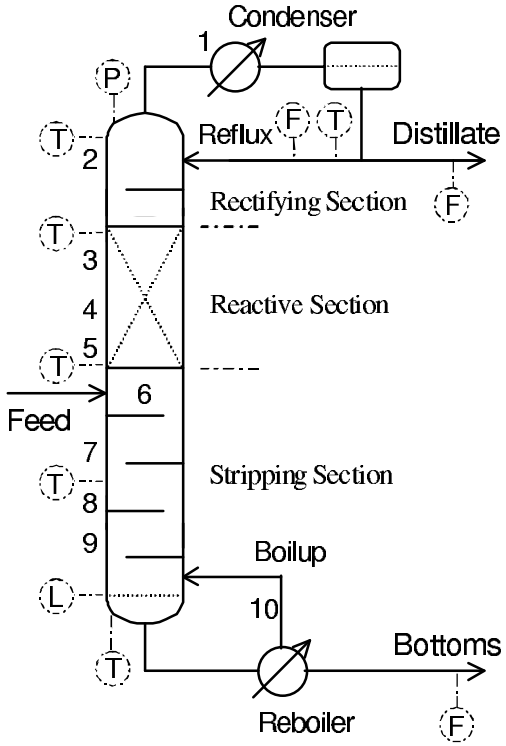

Fig. 1. Pilot-scale RD column (T, F, P, L in dashed circles mean measurements for temperature, flow rate, pressure, and level variables).

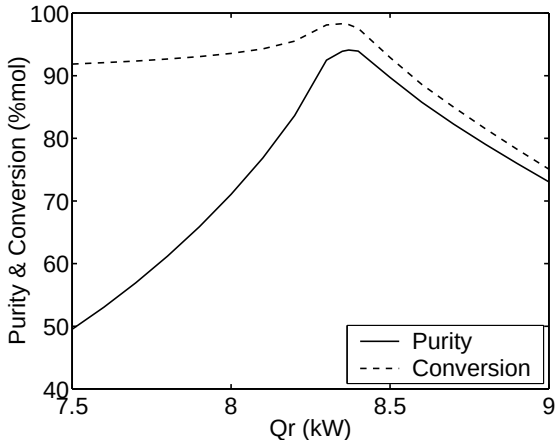

Fig. 2. Purity and Conversion versus reboiler duty for the reflux fixed at 2.53L/min.

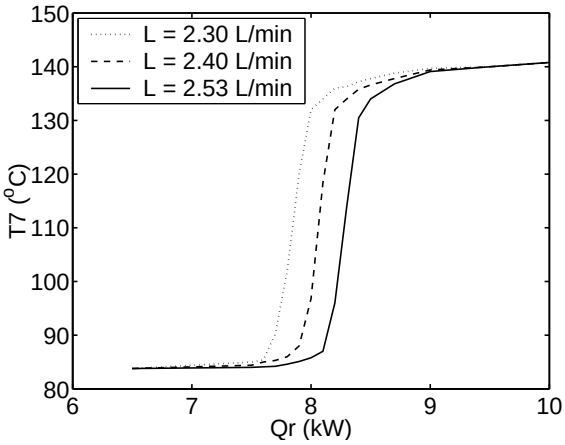

Fig. 3. Stage 7 temperature T_7 versus reboiler duty Q_r.

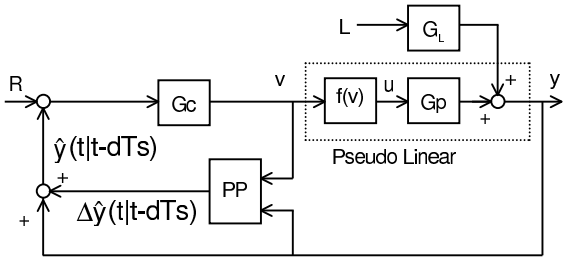

Fig. 4. PPC system structure.

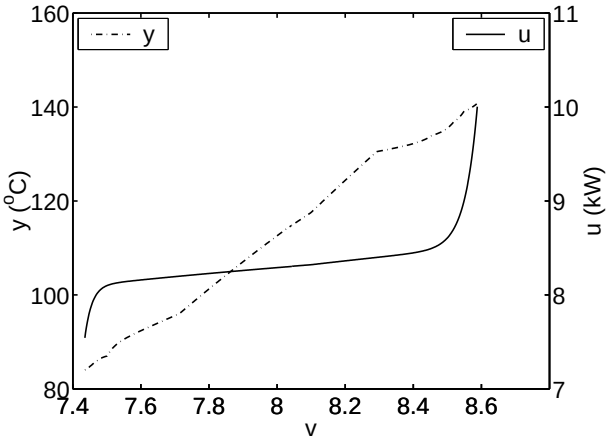

Fig. 5. Nonlinear transformation and the resulting y versus v relationship.

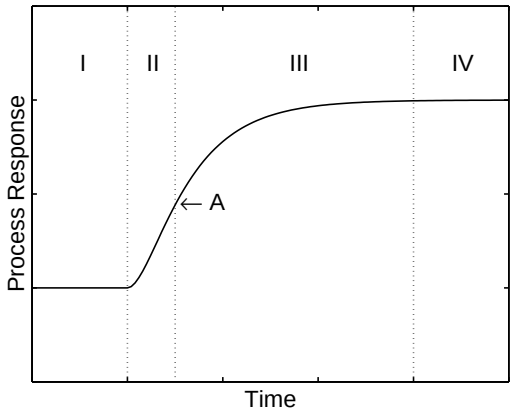

Fig. 6. S-shape process response to a step change in either the manipunated variable or disturbances. I: time delay stage; II: accelerating increase stage; III: decelerating increase stage; IV: steady state stage; A: inflection point.

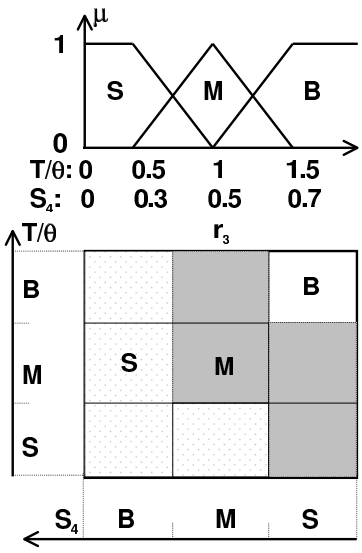

Fig. 7. Fuzzy sets and fuzzy rules.

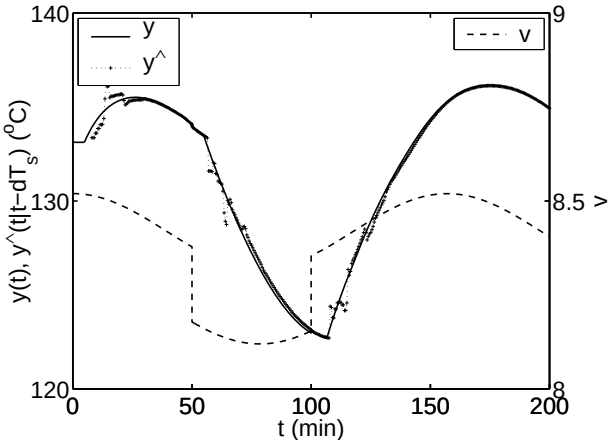

Fig. 8. Typical curves of v, y, and $\hat{y}$.

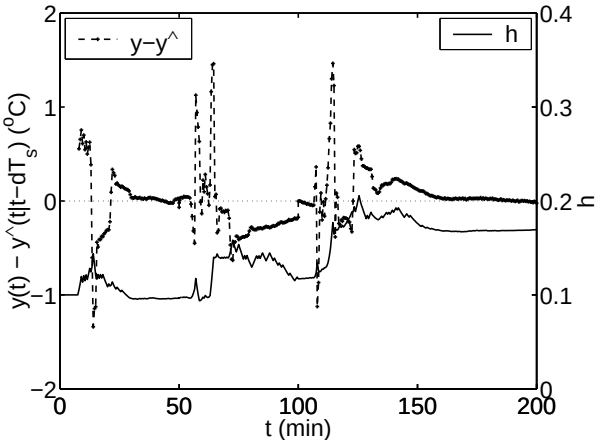

Fig. 9. Typical $y(t) - \hat{y}(t|t - dT_s)$ and h curves corresponding to Figure 8.

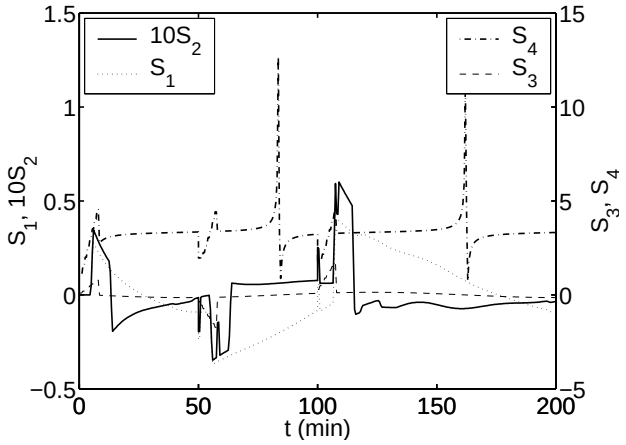

Fig. 10. Typical curves of S_1 to S_4 corresponding to Figure 8.

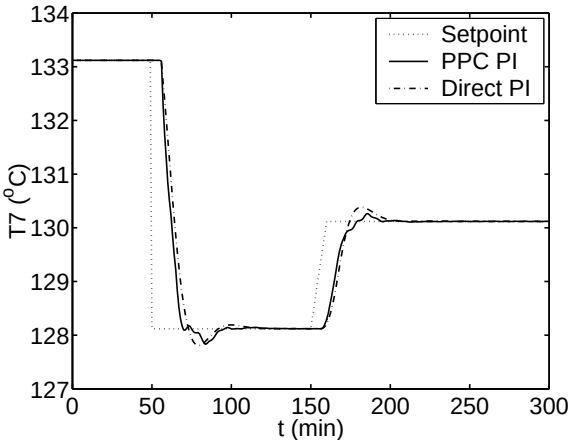

Fig. 11. Setpoint tracking.

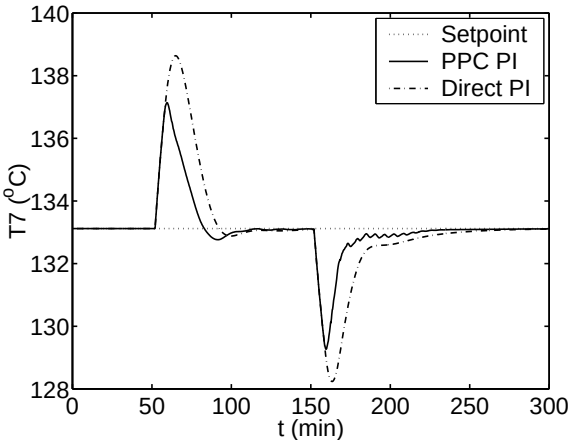

Fig. 12. Rejection of ±5% disturbances in feed composition.

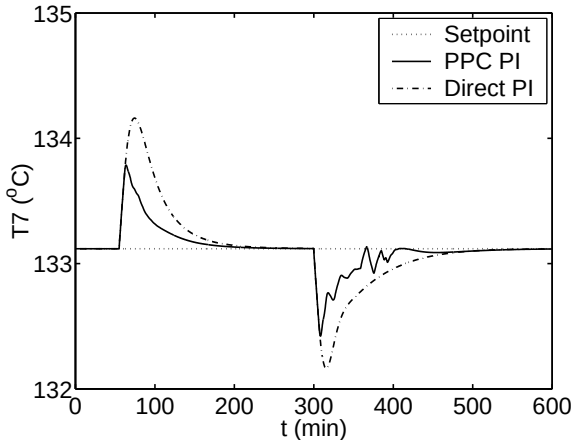

Fig. 13. Rejection of $\mp 10\%$ disturbances in feed flow rate.